



universität  
wien

# BACHELORARBEIT

Titel der Bachelorarbeit

Bell's theorem and experimental tests

Verfasser

Cheng Xiayi

Matrikelnummer: a0800812

Institut für Experimentalphysik der Universität Wien

angestrebter akademischer Grad

Bachelor of Science (B. Sc.)

Wien, im Juli 2011

Studienkennzahl lt. Studienblatt: 033676

Betreuer: Ao. Univ. -Prof. Dr. Reinhold A. Bertlmann

# Contents

<b>1</b>	<b>Introduction</b>	<b>3</b>
<b>2</b>	<b>Basic concepts of quantum mechanics</b>	<b>5</b>
2.1	The density operator . . . . .	7
2.2	The entangled state . . . . .	8
<b>3</b>	<b>Part I: Bell's Theorem</b>	<b>9</b>
3.1	Bell's Theorem . . . . .	9
3.2	The general argument (1964) . . . . .	11
3.3	CHSH – The non-idealized case (1971) . . . . .	13
3.4	CH – more experiment related (1974) . . . . .	15
3.5	Wigner – a combinatorial analysis . . . . .	17
3.6	Relations between Bell's inequality and entanglement witness	18
<b>4</b>	<b>Part II: Experimental Tests</b>	<b>20</b>
4.1	Requirement for general experimental tests . . . . .	20
4.2	The “First” Generation . . . . .	22
4.3	The “Second” Generation . . . . .	24
4.4	The “Third” Generation - G. Weihs, A. Zeilinger 1998 . . . . .	27
4.5	Lab report . . . . .	29
4.5.1	Experimental requirements . . . . .	29
4.5.2	Setup and execution . . . . .	29
4.5.3	Results . . . . .	33
4.5.4	Discussion . . . . .	36
<b>5</b>	<b>Conclusion</b>	<b>37</b>
<b>6</b>	<b>Acknowledgement</b>	<b>38</b>

# Chapter 1

## Introduction

We can say that one of the greatest philosophical and physical discussions was caused by a single paper written by Einstein, Podolsky and Rosen[1] (EPR) in 1935<sup>1</sup>. In the paper, EPR assume reasonably the non-existence of the action-at-distance and define the criteria for a complete physical theory, which include the concepts of local causality and physical reality. By demonstrating mathematically their ideas within a thought experiment, which was modified by Bohm[26] later on, they concluded that the description of quantum mechanics may be incomplete. This conclusion is formulated because this real, deterministic property isn't contained in the formalism of quantum theory. And that is also the birth of the term of the "spooky action at the distance[1]." The observation on one system immediately influences the observation on the second one.

Few months later, Bohr[2] replied to EPR and defended quantum mechanics with his principle of complementarity. He denoted that the realistic viewpoint is inapplicable under the macroscopic level.

In the following decades, in order to fulfill the desire of understanding nature, not only was the validation of contextuality in nature questioned, but also the suggestions of extending quantum physics with a model of unknown "hidden" variable theory (HVT) for the completion were proposed. Many great physicists, e.g. Von Neumann, Gleason, Jauch and Piron, made some attempts to deny the theoretical extension. Apparently, all the proofs contain some leakages in their axioms or failed at the point of determinism and congruence with quantum mechanics[3].

Finally, both possible explanations were fully eliminated by the two following "no-go" theorems: the Kochen-Specker theorem and Bell's theorem.

The present work covers Bell's theorem, published in 1964[4] by John Bell. He formulates a contradiction between the HVT and quantum mechanical

---

<sup>1</sup>Interestingly, the EPR paper became cited with a delay of 30 years, i.e., after Bell published his inequality and nowadays in the age of quantum information, there is an exponential increase of citations.

measurement. Besides the brief summaries of a few interesting proofs of Bell's theorem, the most significant historical experimental tests of Bell's theorem, during the last decades, are hereby also described and analysed.

## Chapter 2

# Basic concepts of quantum mechanics

In this chapter, a short introduction into quantum mechanics will be explained and all necessary mathematical notations for understanding the present work will also be mentioned.

According to the fundamental law of quantum mechanics, a quantum state  $\phi$  of a given system is described by a complex function, called the wave function, which contains the complete knowledge of the state and allows one to determine the probabilities of obtaining certain measurement results made in the state. Suppose  $\phi(\vec{x}, t)$  is a function of the space  $\vec{x}$  and time  $t$ , then the probability of finding the system in the coordinate interval  $[\vec{x}, \vec{x} + d\vec{x}]$  or shortly  $d^3x$  at time  $t$  is given by

$$|\phi(\vec{x}, t)|^2 d^3x \quad (2.1)$$

And due to the normalization condition, the total probability is:

$$\|\phi\|^2 = \int |\phi(\vec{x}, t)|^2 d^3x = 1 = \langle\phi|\phi\rangle \quad (2.2)$$

where  $\|\cdot\| = \sqrt{\langle\cdot|\cdot\rangle}$  and the right side of the equation is expressed by the Dirac notation.

To gain a deeper understanding of the quantum states, let us consider the space underlying our physical objects, which is also called the Hilbert space.

**Definition:** A Hilbert space  $H$  is a finite- or infinite-dimensional, linear vector space with the scalar product in  $C$  (Complex field). The inner product of the elements of the space,  $\langle\phi|\psi\rangle = \int \phi^* \psi d^3x$ , with  $\phi, \psi \in H$ , satisfies the following properties, where  $\phi^*$  is the complex conjugate of  $\phi$ :

- $\langle\phi|\psi\rangle$  is complexly conjugated:

$$\langle\phi|\psi\rangle = \overline{\langle\psi|\phi\rangle}$$

where the term with overline denotes the complex conjugation.

- $\langle \phi | \psi \rangle$  is linear in its second argument. For all complex number  $a$  and  $b$ :

$$\langle \phi | a\psi_1 + b\psi_2 \rangle = a\langle \phi | \psi_1 \rangle + b\langle \phi | \psi_2 \rangle$$

- The inner product is positive definite:

$$\langle \phi | \phi \rangle \geq 0$$

where the case of equality holds for  $\phi = 0$ .

- The norm, a real-value function, is also defined by the inner product:

$$\|\phi\| = \sqrt{\langle \phi | \phi \rangle}$$

Physical states expressed by wave functions obey the superposition principles. If  $\{|\phi_i\rangle\}$  are all possible states of  $H$ , then any linear combination  $|\phi\rangle$  of them also belongs to  $H$ :

$$|\phi\rangle = c_1|\phi_1\rangle + c_2|\phi_2\rangle + \dots + c_N|\phi_N\rangle \quad (2.3)$$

where  $\{c_i\}$  are complex numbers and  $i = 1, 2, \dots, N$ .  $|c_i|^2$  gives the probability of obtaining  $\phi_i$  with  $\sum_{i=1}^N |c_i|^2 = 1$ :

$$|c_i|^2 = |\langle \phi_i | \psi \rangle|^2 \quad (2.4)$$

If  $\{|\phi_i\rangle\}$  are orthonormal, they are called the orthonormal bases. Therefore a quantum state can be generally written as:

$$|\phi\rangle = \sum_{i=1}^N c_i |\phi_i\rangle \quad (2.5)$$

The observables are operators which act on the wave function, if certain physical quantities need to be measured. The measurement results are given by the eigenstates of the corresponding observable with their eigenvalues. Imagine an operator  $A$  acting on any arbitrary eigenstate  $|\phi_i\rangle$ , then:

$$A|\phi_i\rangle = \lambda_i |\phi_i\rangle$$

where  $\lambda_i$  is the eigenvalue and denotes the measurement probability.

The most important analysis of this work is based on the expectation value of an observable. Since a statistical average value for the given observable acted on a large number of the identically prepared systems is required, this mean value is defined by the expectation value:

$$\langle A \rangle_\phi = \int \phi^* A \phi d^3x = \langle \phi | A | \phi \rangle = \sum_{n,p=0}^N c_n^\dagger c_p A_{n,p} \quad (2.6)$$

where  $A_{n,p} = \langle \phi_n | A | \phi_p \rangle$  is the matrix element of the observable  $A$ .

## 2.1 The density operator

Usually, we often deal with states of systems, which are not perfectly determined. In order to make the maximal use of this partial information we possess about the state of the system, the density matrix formalism is introduced. The density operator  $\rho$  is therefore defined as:

$$\rho = |\phi\rangle\langle\phi| \quad (2.7)$$

Analogously, the expectation value is given by:

$$\langle A \rangle_\phi = \text{tr}(\rho \cdot A) = \text{tr}(A \cdot \rho) \quad (2.8)$$

And

$$\text{tr}(\rho) = 1 \quad (2.9)$$

For a given pure state  $|\phi\rangle$  whose information is perfectly known, the density operator has to fulfil the following properties:

$$\begin{aligned} \rho^2 &= \rho \\ \rho^\dagger &= \rho \\ \text{tr}(\rho^2) &= 1 \end{aligned}$$

For the completeness, a mixed state is present when there is a statistical distribution of pure states. Since there is no interference effects between the pure states, a mixed state can therefore only be given by the density operator:

$$\rho = \sum_i p_i |\phi_i\rangle\langle\phi_i| = \sum_i p_i \rho_i \quad (2.10)$$

where  $\sum_i p_i = 1$  and  $\{p_i\}$  are the probabilities of detecting  $\{|\phi_i\rangle\langle\phi_i|\}$ . The following properties will be satisfied:

$$\begin{aligned} \text{tr}(\rho) &= \sum_i p_i \text{tr}(\rho_i) \\ \text{tr}(\rho) &= 1 \\ \langle A \rangle_\phi &= \text{tr}(\rho \cdot A) \\ \rho^2 &\neq \rho \\ \text{tr}(\rho^2) &\leq 1 \end{aligned}$$

Here the last inequality can be seen as a measure of the mixedness of a given state.

## 2.2 The entangled state

Before starting with Bell's theorem, let us first take a brief look at the entangled state.

We consider the following quantum state vector:

$$|\Phi\rangle = a \cdot |x\rangle_1 |y\rangle_2 + b \cdot e^{-i\phi} \cdot |y\rangle_1 |x\rangle_2 \quad (2.11)$$

which is a general form of an entangled state for two subsystems. Here,  $|a|^2$  and  $|b|^2$  are the probabilities of the corresponding product states  $|x\rangle_1 \otimes |y\rangle_2 = |x\rangle_1 |y\rangle_2$  and  $|y\rangle_1 \otimes |x\rangle_2 = |y\rangle_1 |x\rangle_2$  with  $|a|^2 + |b|^2 = 1$ , the term  $e^{-i\phi}$  denotes a phase difference.

The peculiar property of this kind of states is that they can't be factorized into a product of two states of individual subsystems.

In other words, a state vector  $|\Psi\rangle$  in biparticle system describing, e.g., two subsystems of photons can generally be written in the form:

$$|\Psi\rangle = \sum_{m,n} c_{m,n} |m\rangle_1 |n\rangle_2 \quad (2.12)$$

where  $c_{m,n} = a_m \cdot b_n$  are the probability coefficients of  $|m\rangle_1 |n\rangle_2$ ,  $a_m$  is the  $m$ -th probability coefficient of the single photon state  $|\Psi_1\rangle = \sum_m a_m |m\rangle$ , the analogous notation  $b_n$  for the other single photon.

A state which can be written in Eq. (2.12) is called separable. Otherwise, the state is said to be entangled, which means:

$$c_{m,n} \neq a_m \cdot b_n \quad (2.13)$$

In conclusion, an entangled state can only be totally examined as a whole system. Therefore we define an entangled state as such a state with two or more subsystems, separated by a certain distance, *that the whole system, but not the individual subsystems, is well defined.*

The most remarkable entangled states are called Bell states, which have maximal entanglement and are given for photons with horizontal and vertical polarizations by:

$$|\Psi^+\rangle = \frac{1}{\sqrt{2}}(|H\rangle_1 |V\rangle_2 + |V\rangle_1 |H\rangle_2) \quad (2.14)$$

$$|\Psi^-\rangle = \frac{1}{\sqrt{2}}(|H\rangle_1 |V\rangle_2 - |V\rangle_1 |H\rangle_2) \quad (2.15)$$

$$|\Phi^+\rangle = \frac{1}{\sqrt{2}}(|H\rangle_1 |H\rangle_2 + |V\rangle_1 |V\rangle_2) \quad (2.16)$$

$$|\Phi^-\rangle = \frac{1}{\sqrt{2}}(|H\rangle_1 |H\rangle_2 - |V\rangle_1 |V\rangle_2) \quad (2.17)$$

# Chapter 3

## Part I: Bell's Theorem

### 3.1 Bell's Theorem

Let us consider the following thought experiment made by Bohm[26] (EPRB). Suppose there is a source which is able to make pairs of particles with correlated property. Let's say that the correlation is applied to their spins. Each particle has a spin of one half, but they do have a total spin of zero with an antisymmetric wave function, also called a singlet state, which is given by the following Dirac notation:

$$|\psi^-\rangle = \frac{1}{\sqrt{2}}(|\uparrow\rangle|\downarrow\rangle - |\downarrow\rangle|\uparrow\rangle) \quad (3.1)$$

These particles are sent into reverse directions. When the particles are remote from one other, they will be detected by Stern-Gerlach apparatuses, which simply deflect particles with a corresponding spin “up”-wards or “down”-wards by the established inhomogeneous magnet field, whose orientations are freely adjustable, as shown in Fig. 3.1.

The singlet state defined above simply describes that the possibility of measuring “up” in the detector system 1 and “down” in the system 2 is equal to the possibility of vice versa, if the magnet fields of both apparatuses are chosen to be parallel, e.g., to the z-axis.

The perfect anti-correlation in this case leads us to suggest that the fundamental laws of physics are deterministic. The “stochastic” measurement results are the results of imperfect experimental setups. Therefore it was very reasonable to propose such a deterministic, unknown model to describe the quantum world, since this pre-determinism has not be considered in the quantum mechanical description. The only necessary property of these hidden variable theories is the agreement between theoretical prediction and the statistical reality. In the present chapter, we will discuss whether it is possible to prove the existence of such theories with the latter requirement. First of all, let us analyze the correlation concerning the measurement of

EPRB experiment. Let us give the measurement results actual values of 1 for photon deflected “up” and -1 for “down.” This correlation is indeed nothing major in the case of parallel magnet field orientations. But what happens when the fields are rotated by arbitrary angles  $\alpha$  and  $\beta$  respectively for systems 1 and 2? In other words, what is the correlation if the fields are randomly orientated?

If the measurement is repeated N times, from a classical point of view, we

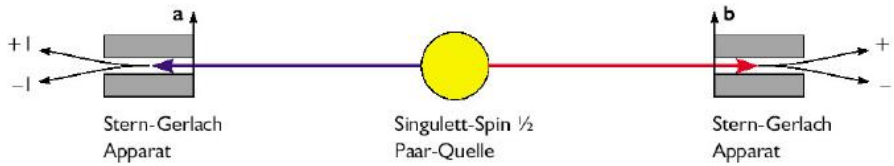


**Figure 3.1:** EPRB thought experiment with Stern Gerlach apparatuses (Ref. [22])

will receive a correlation:

$$\langle ab \rangle_{\psi^-} = \sum_j \frac{a_j b_j}{N} \quad (3.2)$$

where  $a_j$  and  $b_j$  are separately the measurement results in systems 1 and 2. A geometric illustration for this classic correlation is to image an unit vector representing the magnet field orientation in system 1, let us call it  $\vec{\alpha}$ , and the analogous notation  $\vec{\beta}$  for system 2. Suppose the planes, which  $\vec{\alpha}$  and  $\vec{\beta}$  are separately perpendicular to, are disks, as shown in Fig. 3.2. From Eq.

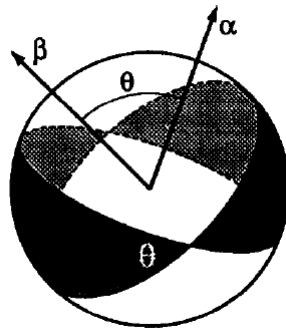


**Figure 3.2:** The two disks divide the unit sphere into 4 parts, which represent the correlation between the measurements. The shaded areas can be interpreted as anti-correlation, while the rest as correlation. (Ref. [9])

(3.2) we obtain the classical correlation:

$$\langle ab \rangle_{\psi^-} = \frac{\theta - (\pi - \theta)}{\pi} = -1 + \frac{2\theta}{\pi} \quad (3.3)$$

Let us now return to the statistical prediction of quantum mechanics. The measurements of each particle are done by the observables  $\vec{\alpha}\vec{\sigma}_1$  and  $\vec{\beta}\vec{\sigma}_2$ , respectively. Hence, the correlation is given by:

$$\langle ab \rangle_{\psi^-} = \langle \vec{\alpha}\vec{\sigma}_1 \otimes \vec{\beta}\vec{\sigma}_2 \rangle_{\psi^-} = -\vec{\alpha}\vec{\beta} = -\cos\theta \quad (3.4)$$

where  $\theta$  is the angle difference between the  $\vec{\alpha}$  and  $\vec{\beta}$  and the  $\sigma$  are the Pauli matrices.

We see Eq. (3.3) only partially reproduces quantum mechanical results of Eq. (3.4) at  $\theta = 0$ ;  $\pi/2$  and  $\pi$ .

This is one of the very first peculiar examples concerning the difference between local, deterministic theories and statistical prediction of quantum mechanical theories.

## 3.2 The general argument (1964)

Actually, from Eq. (3.4) we are able to calculate the quantum mechanical prediction for the expectation value of the observable  $\vec{\alpha}\vec{\sigma}_1 \otimes \vec{\beta}\vec{\sigma}_2$ :

$$[E(\vec{\alpha}, \vec{\beta})]_{\psi^-} = \langle \vec{\alpha}\vec{\sigma}_1 \otimes \vec{\beta}\vec{\sigma}_2 \rangle_{\psi^-} = -\vec{\alpha}\vec{\beta} \quad (3.5)$$

One critical assumption, which Bell's derivation relies on, is the special case of Eq. (3.5):

$$[E(\vec{\alpha}, \vec{\alpha})]_{\psi^-} = -1 \quad (3.6)$$

which contains the deterministic property of this idealized system that the detected samples have to be perfectly correlated.

Since a local, realistic interpretation of quantum mechanics is requested, but a quantum state can't be determined for an individual measurement, one has to assume a more advanced specification, in which the determinism is built.

In this case, Bell introduced a "hidden" variable  $\lambda$ , which he hasn't made any restriction for, either in its dimension or in its construction. Properties of this will be demonstrated below:

If we repeat the spin measuring in the given thought experiment, we will see the unsurprisingly correlated results. The possibility  $P(A, B|\vec{\alpha}, \vec{\beta})$  that A as measured result in system 1 with field orientation  $\vec{\alpha}$  and B in system 2 with  $\vec{\beta}$ , can't be factorized into  $P_1(A, \vec{\alpha}) \cdot P_2(B, \vec{\beta})$ . That means that a certain correlation can't be locally explained without "action-at-a-distance".

By applying  $\lambda$ , we claim the following:

$$P(A, B|\vec{\alpha}, \vec{\beta}, \lambda) = P_1(A, \vec{\alpha}, \lambda) \cdot P_2(B, \vec{\beta}, \lambda) \quad (3.7)$$

This is a hypothesis of local causality or “no-action-at-distance”. In order to make this local theory congruent with quantum mechanical results,  $\lambda$  is introduced. Therefore this variable, which we don't know, can be seen as a supplement for quantum mechanics. In order to define the probability of measurements for an ensemble, Bell defined intuitively the distribution function for  $\lambda$ :

$$\int d\lambda \rho(\lambda) = 1 \quad (3.8)$$

If  $\rho(\lambda)$  is a normalized probability distribution, the expectation value of a joint spin measurement at  $\vec{\alpha}$  and  $\vec{\beta}$  can be written as:

$$E(\vec{\alpha}, \vec{\beta}) = \int \rho(\lambda) A(\vec{\alpha}, \lambda) B(\vec{\beta}, \lambda) d\lambda \quad (3.9)$$

where  $A(\vec{\alpha}, \lambda) = \pm 1$  and  $B(\vec{\beta}, \lambda) = \pm 1$ .

According to the conditions of the hidden-variable theory, the above equation has to be equal to Eq. (3.5). From Eq. (3.6),

$$A(\vec{\alpha}, \lambda) = -B(\vec{\alpha}, \lambda) \quad (3.10)$$

has to hold. Assuming the correctness of Eq. (3.9), we obtain Eq. (3.11) by substituting Eq. (3.10) into Eq. (3.9):

$$E(\vec{\alpha}, \vec{\beta}) = - \int \rho(\lambda) A(\vec{\alpha}, \lambda) A(\vec{\beta}, \lambda) d\lambda \quad (3.11)$$

By introducing a third field orientation  $\vec{\gamma}$ , we have

$$\begin{aligned} & E(\vec{\alpha}, \vec{\beta}) - E(\vec{\alpha}, \vec{\gamma}) \\ &= - \int \rho(\lambda) [A(\vec{\alpha}, \lambda) A(\vec{\beta}, \lambda) - A(\vec{\alpha}, \lambda) A(\vec{\gamma}, \lambda)] d\lambda \\ &= - \int \rho(\lambda) A(\vec{\alpha}, \lambda) A(\vec{\beta}, \lambda) [1 - A(\vec{\beta}, \lambda) A(\vec{\gamma}, \lambda)] d\lambda \end{aligned} \quad (3.12)$$

Since  $A, B = \pm 1$ , the equation above turns to the following inequality:

$$|E(\vec{\alpha}, \vec{\beta}) - E(\vec{\alpha}, \vec{\gamma})| \leq \int \rho(\lambda) [1 - A(\vec{\beta}, \lambda) A(\vec{\gamma}, \lambda)] d\lambda \quad (3.13)$$

And finally,

$$|E(\vec{\alpha}, \vec{\beta}) - E(\vec{\alpha}, \vec{\gamma})| \leq 1 + E(\vec{\beta}, \vec{\gamma}) \quad (3.14)$$

This is the original form of Bell's inequality.

If a theory described by a local, deterministic hidden variable is true, the inequality above will hold. But a simple test by using Eq. (3.5) and taking  $\vec{\alpha}, \vec{\beta}$  and  $\vec{\gamma}$  to be coplanar as well as taking account of the following conditions:

$$\begin{aligned} \vec{\alpha} \cdot \vec{\beta} &= \vec{\beta} \cdot \vec{\gamma} = \frac{1}{2} \\ \vec{\alpha} \cdot \vec{\gamma} &= -\frac{1}{2} \end{aligned} \quad (3.15)$$

leads to a mathematical contradiction:

$$|E(\vec{\alpha}, \vec{\beta}) - E(\vec{\alpha}, \vec{\gamma})| = 1 \leq \frac{1}{2} = 1 + E(\vec{\beta}, \vec{\gamma}) \quad (3.16)$$

This version of Bell's theorem, as just proved, can be summarized as follows: ***No deterministic hidden-variable theory satisfying Eq. (3.6) and the locality condition Eq. (3.9), can agree with all of the predictions by quantum mechanics concerning the spin of a pair spin- $\frac{1}{2}$  particles in the singlet state.***<sup>1</sup>

### 3.3 CHSH – The non-idealized case (1971)

A physical theory can't be considered valid as long as it is not proven experimentally. The very first Bell's inequality Eq. (3.14) describes the idealized case, which strongly depends on Eq. (3.6). In fact, this condition can't hold for actual experiments because any state analyzer will always have some leakages for some reason. Therefore it is outrageously difficult to be realized in the lab. Exactly these problems are approached by Clauser, Horne, Shimony and Holt[5] (CHSH), who extended the Bell's inequality for the non-deterministic case, which doesn't depend on the mentioned critical condition Eq. (3.6).

Here the measurement results  $A(\vec{\alpha}, \lambda)$  and  $B(\vec{\beta}, \lambda)$  in systems 1 and 2 were respectively assigned as the following:

$$|A(\vec{\alpha}, \lambda)| \leq 1 \quad (3.17)$$

$$|B(\vec{\beta}, \lambda)| \leq 1$$

$\leq 1$  also includes the non-idealized case, when +1 for detecting "up", -1 for "down" and 0 for blank.

The locality condition is still included in the expectation values given in Eq. (3.9). Now consider the following expression:

$$E(\vec{\alpha}, \vec{\beta}) - E(\vec{\alpha}, \vec{\beta}') = \int \rho(\lambda)[A(\vec{\alpha}, \lambda)B(\vec{\beta}, \lambda) - A(\vec{\alpha}, \lambda)B(\vec{\beta}', \lambda)]d\lambda$$

This can be written as:

$$E(\vec{\alpha}, \vec{\beta}) - E(\vec{\alpha}, \vec{\beta}') = \int \rho(\lambda)A(\vec{\alpha}, \lambda)B(\vec{\beta}, \lambda)[1 \pm A(\vec{\alpha}', \lambda)B(\vec{\beta}', \lambda)]d\lambda - \int \rho(\lambda)A(\vec{\alpha}, \lambda)B(\vec{\beta}', \lambda)[1 \pm A(\vec{\alpha}', \lambda)B(\vec{\beta}, \lambda)]d\lambda$$

---

<sup>1</sup>J. F. Clauser, A. Shimony, Rep.Prog.Phys. 41 1881 (1978)

where  $\vec{\alpha}$ ,  $\vec{\alpha}'$ ,  $\vec{\beta}$  and  $\vec{\beta}'$  are all different field orientations. By applying Eq. (3.17) and the triangle inequality, we have:

$$|E(\vec{\alpha}, \vec{\beta}) - E(\vec{\alpha}, \vec{\beta}')| \leq$$

$$\int \rho(\lambda)[1 \pm A(\vec{\alpha}', \lambda)B(\vec{\beta}', \lambda)]d\lambda + \int \rho(\lambda)[1 \pm A(\vec{\alpha}', \lambda)B(\vec{\beta}, \lambda)]d\lambda$$

or

$$|E(\vec{\alpha}, \vec{\beta}) - E(\vec{\alpha}, \vec{\beta}')| \leq \pm|E(\vec{\alpha}', \vec{\beta}') + E(\vec{\alpha}', \vec{\beta})| + 2$$

Therefore the CHSH inequality is:

$$|E(\vec{\alpha}, \vec{\beta}) - E(\vec{\alpha}, \vec{\beta}')| + |E(\vec{\alpha}', \vec{\beta}) + E(\vec{\alpha}', \vec{\beta}')| \leq 2 \quad (3.18)$$

Mathematically, this inequality can be easily violated if we take the four vectors above to be coplanar with an included angle of  $\pi/4$ . Hence, the quantum mechanical limit of violation of Bell's inequality is given by:

$$|E(\vec{\alpha}, \vec{\beta}) - E(\vec{\alpha}, \vec{\beta}')| + |E(\vec{\alpha}', \vec{\beta}) + E(\vec{\alpha}', \vec{\beta}')| = 2\sqrt{2} \quad (3.19)$$

$$2\sqrt{2} > 2$$

On the other hand, if the condition of perfect correlation Eq. (3.6) holds, CHSH Eq. (3.19) implies the original Bell's inequality Eq. (3.14) as a special case.

Surely, CHSH inequality isn't the universal solution of all problems. Generally, the following four different cases of the observation are possible when detecting particles passing through some analyzer: a) both particles are observed, b) only particle one is observed, c) only particle two is observed, d) none of them are observed. Clearly, the probability density distribution  $\rho$  of the union of these four sub-ensembles is independent of setting angles  $\vec{\alpha}$  and  $\vec{\beta}$  of the analyzers, but on the collimator and source geometry. However, the mode of partitioning of the measurement results may well depend on the angle. Therefore there is no reason to assume that the composition and distribution of each sub-ensemble has no angle dependence.

Since the normalization of  $\rho$ , see Eq. (3.8) is used in the derivation, the expectation of the independence of  $\vec{\alpha}$  and  $\vec{\beta}$  of  $\rho$  has to be made. Therefore the ensemble for which  $\rho$  is defined must also include unobserved particles. Because the number of unobserved particles is unknown, a comparison of CHSH with experimental evidence would be inadequate. Exactly, this fact is considered by Clauser and Horne[6], which will be discussed in the next chapter. They derived an inequality from the hypothesis of locality and determinism or realism, in which only the ratios of the detection properties are used and the crucial condition of Eq. (3.8) is not required.

### 3.4 CH – more experiment related (1974)

Clauser and Horne[6] (CH) found another inequality, which has a weaker assumption than CHSH. Therefore it is performable in an actual experiment. First of all, consider the apparatus configuration given in Fig. 3.3 Suppose the adjustable values for the orientations of apparatuses 1 and 2

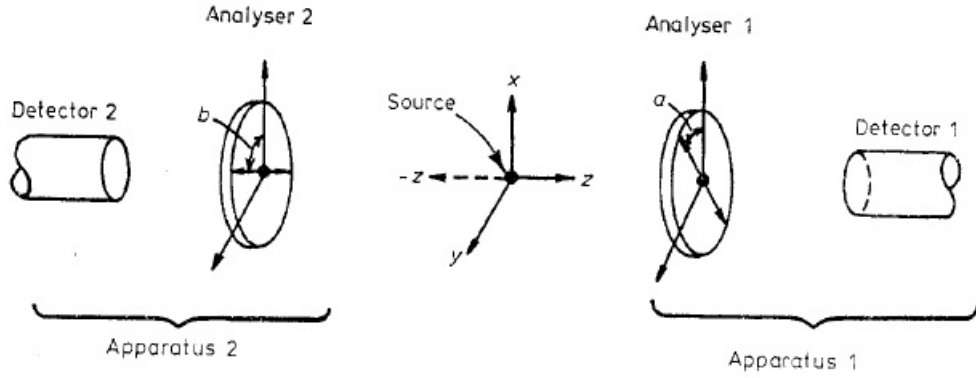


**Figure 3.3:** The basic idea of an experiment on Bell's theorem: The source emits a pair of correlated particles, which are analyzed by two apparatuses. Each apparatus consists of an analyzer, whose orientation is adjustable, and a detector, which is able to measure the rate of the counts. Comparing both measurement results yields the number of coincidence. (Ref. [10])

are described by  $\alpha$  and  $\beta$  respectively. Suppose  $N$  is the total number of paired correlated particles emitted by the source, during a given integration time.  $N_1(\alpha)$  and  $N_2(\beta)$  describe separately the number of counts in system 1 with  $\alpha$  and system 2 with  $\beta$ .  $N_{12}(\alpha, \beta)$  is the number of simultaneous detection (coincidence) in system 1 and 2. Further more, the possibilities for these results are given by:

$$\begin{aligned} p_1(\alpha) &= N_1(\alpha)/N \\ p_2(\beta) &= N_2(\beta)/N \\ p_{12}(\alpha, \beta) &= N_{12}(\alpha, \beta)/N \end{aligned} \tag{3.20}$$

if  $N$  is sufficiently large.

By applying the hidden variable  $\lambda$ , we assume that  $\alpha$ ,  $\beta$ ,  $\lambda$ ,  $p_1$  and  $p_2$  are independent and we also demand the following relation:

$$p_{12}(\alpha, \beta, \lambda) = p_1(\alpha, \lambda) \cdot p_2(\beta, \lambda) \tag{3.21}$$

The averaged probabilities above are then intuitively given by:

$$\begin{aligned}
p_1(\alpha) &= \int \rho(\lambda)p_1(\alpha, \lambda)d\lambda \\
p_2(\beta) &= \int \rho(\lambda)p_2(\beta, \lambda)d\lambda \\
p_{12}(\alpha, \beta) &= \int \rho(\lambda)p_1(\alpha, \lambda)p_2(\beta, \lambda)d\lambda
\end{aligned} \tag{3.22}$$

which are then not depended on the unknown variable.

After using the lemma<sup>2</sup> proved by Clauser and Horne[6] and the assumption:

$$0 \leq p_i(\lambda, \alpha) \leq p_i(\lambda, \infty) \leq 1 \tag{3.24}$$

which denotes that the probability of detecting a photon after a polarizer is always less or equal to the case with the removed analyzer, the inequality can be written in the following:

$$\begin{aligned}
-p_{12}(\infty, \infty) &\leq p_{12}(\lambda, \alpha, \beta) - p_{12}(\lambda, \alpha, \beta') \\
&\quad + p_{12}(\lambda, \alpha', \beta) + p_{12}(\lambda, \alpha', \beta') \\
&\quad - p_{12}(\lambda, \alpha', \infty) - p_{12}(\lambda, \infty, \beta) \leq 0
\end{aligned} \tag{3.25}$$

After averaging and building the ratio of probabilities, we receive the CH-inequality:

$$\begin{aligned}
&\frac{p_{12}(\alpha, \beta) - p_{12}(\alpha, \beta') + p_{12}(\alpha', \beta) + p_{12}(\alpha', \beta')}{p_{12}(\alpha', \infty) + p_{12}(\infty, \beta)} \\
&= \frac{R(\alpha, \beta) - R(\alpha, \beta') + R(\alpha', \beta) + R(\alpha', \beta')}{R_{12}(\alpha', \infty) + R_{12}(\infty, \beta)} \leq 1
\end{aligned} \tag{3.26}$$

where R denotes the rate of counts of coincidence, which is proportional to the number of detected particles, and terms including  $\infty$  stand for the coincidence rate of detection when the corresponding analyzer is removed. As we see, the assumption that the total number N of emitted particles is in this case irrelevant, rules out one of the practical impossibilities of detection. In order to complete the proof of the theorem, let us consider, e.g., the detection of spin-correlated photons given in Eq. (2.16) with linear polarizers. By introducing the quantum mechanical probability into the CH-inequality,

$$\begin{aligned}
p_{12}^{qm}(\alpha, \beta) &= |[(\langle 1|H|\cos\alpha + \langle 1|V|\sin\alpha) \otimes (\langle 2|H|\cos\beta + \langle 2|V|\sin\beta)] \cdot \\
&\quad \frac{1}{\sqrt{2}}[|H\rangle_1|H\rangle_2 + |V\rangle_1|V\rangle_2]|^2 \\
&= \frac{1}{4}(1 + \cos 2(\beta - \alpha))
\end{aligned} \tag{3.27}$$

---

<sup>2</sup>if  $x, x', y, y', X, Y$  are real numbers such that  $0 \leq x, x' \leq X$  and  $0 \leq y, y' \leq Y$ , then the inequality:

$$-XY \leq xy - xy' + x'y + x'y' - Yx' - Xy \leq 0 \tag{3.23}$$

holds.

where  $\alpha$  and  $\beta$  are the angles of the polarizers. The probability of detecting one photon is simply  $\frac{1}{2}$ . By choosing  $\alpha = 0^\circ$ ,  $\beta = 22.5^\circ$ ,  $\alpha' = 45^\circ$  and  $\beta' = 65.5^\circ$ , the violation yields out:

$$p_{12}^{qm}(\alpha, \beta) - p_{12}^{qm}(\alpha, \beta') + p_{12}^{qm}(\alpha', \beta) + p_{12}^{qm}(\alpha', \beta') - p_1^{qm}(\alpha') - p_2^{qm}(\beta) = \frac{\sqrt{2} - 1}{2} \leq 0 \quad (3.28)$$

which is clearly a contradiction.

By adding symmetry consideration from quantum mechanical predictions the CH-inequality can be specified for the following conditions:

$$\begin{aligned} p_1(\alpha) &= \text{const.} \\ p_2(\beta) &= \text{const.} \\ p_{12} &= f(|\beta - \alpha|) \end{aligned}$$

and after choosing:

$$|\alpha - \beta| = |\alpha' - \beta'| = |\alpha' - \beta| = \frac{1}{3}|\alpha - \beta'| = \phi$$

we receive the following inequality given by  $S(\phi)$ :

$$S(\phi) \equiv \frac{3p_{12}(\phi) - p_{12}(3\phi)}{p_1 + p_2} \leq 1 \quad (3.29)$$

At first sight, the inequality above seems to be elegant because of the small number of measurements. But the truth is that fulfilling the necessary condition requires many more measurement procedures.

### 3.5 Wigner – a combinatorial analysis

This version of Wigner's inequality is derived by pure combinatorial analysis[7], where perfect anti-correlation and perfect detection efficiency are assumed. Let us first consider the familiar EPR experiment and suppose there are three possible detection parameters such as A, B and C with the possible measurement result of + or -. By assuming the locality condition, we can construct the following combinations of measurement results in Table 3.1. Since the numbers of counts are positive, the following inequality must hold:

$$N_3 + N_4 \leq (N_2 + N_4) + (N_3 + N_7) \quad (3.30)$$

Further, the probability of measuring + in one detector with the setting A and + in the other detector with the setting B is given by:

$$p(A+, B+) = \frac{N_3 + N_4}{N} \quad (3.31)$$

The number of counts	Particle 1	Particle 2
$N_1$	$(A+, B+, C+)$	$(A-, B-, C-)$
$N_2$	$(A+, B+, C-)$	$(A-, B-, C+)$
$N_3$	$(A+, B-, C+)$	$(A-, B+, C-)$
$N_4$	$(A+, B-, C-)$	$(A-, B+, C+)$
$N_5$	$(A-, B+, C+)$	$(A+, B-, C-)$
$N_6$	$(A-, B+, C-)$	$(A+, B-, C+)$
$N_7$	$(A-, B-, C+)$	$(A+, B+, C-)$
$N_8$	$(A-, B-, C-)$	$(A+, B+, C+)$

**Table 3.1:** Possible combinations of measurement results

where  $N = \sum_i^8 N_i$  is the total number of counts. Analogously, we have:

$$p(A+, C+) = \frac{N_2 + N_4}{N}$$

$$p(C+, B+) = \frac{N_3 + N_7}{N}$$

By applying the relations above into Ineq. (3.30), we obtain the Wigner's inequality:

$$p(A, B) \leq p(A, C) + p(C, B) \quad (3.32)$$

Another path of derivation of Wigner's inequality is to make use of the discrete expectation value of correlation, such as:

$$E(A, B) = p(A+, B+) + p(A-, B-) - p(A+, B-) - p(A-, B+) \quad (3.33)$$

where  $\sum_i p_i = 1$ .

A contradiction results, when the probability for correlation is, e.g., given by:

$$p(A, B) = |(\langle A+ | \otimes \langle B+ |) |\psi^-\rangle|^2 = \frac{\sin^2(\frac{\angle(A, B)}{2})}{2} \quad (3.34)$$

and if we chose the following angles:  $\angle(A, B) = 60^\circ$ ,  $\angle(B, C) = 60^\circ$  and  $\angle(A, C) = 120^\circ$ .

### 3.6 Relations between Bell's inequality and entanglement witness

In this last section of the part I, an extended feature of Bell's inequality will be briefly sketched. Let us recall the definition of entangled states. In general, a state in bi-particle system is said to be separable if and only if it can be written as:

$$\rho = \sum_i p_i |\phi_i\rangle_A \langle \phi_i| \otimes |\phi_i\rangle_B \langle \phi_i| \quad (3.35)$$

where  $\sum_i p_i = 1$  and  $0 \leq p_i \leq 1$ . Otherwise the state is entangled. Since this criterion is often very complicated to be tested, many methods are constructed to distinguish between separable and entangled states. One foundational method of quantum entanglement theory is the so-called entanglement witness. It is a Hermitian operator  $W$ , which is defined for separable states  $\rho_{A,B}^{sep}$  by:

$$\text{tr}(\rho_{A,B}^{sep} \cdot W) \geq 0 \quad (3.36)$$

and for entangled states  $\rho_{A,B}^{ent}$  by:

$$\text{tr}(\rho_{A,B}^{ent} \cdot W) < 0 \quad (3.37)$$

According to the fact that separable states do not violate Bell's inequality, one is able to construct an entanglement witness upon the CHSH inequality. Let us first of all represent Eq. (3.19) by

$$\text{tr}(B_{CHSH}\rho) \leq 2 \quad (3.38)$$

where  $B_{CHSH}$  is the CHSH operator defined by

$$B_{CHSH} = \vec{\alpha} \cdot \vec{\sigma} \otimes (\vec{\beta} + \vec{\beta}') \cdot \vec{\sigma} + \vec{\alpha}' \cdot \vec{\sigma} \otimes (\vec{\beta} - \vec{\beta}') \cdot \vec{\sigma} \quad (3.39)$$

with  $\vec{\sigma} = (\sigma_x, \sigma_y, \sigma_z)^T$ . Therefore an entanglement witness  $W_{CHSH}$  basing on the CHSH inequality is given by:

$$W_{CHSH} = 2 \cdot I + B_{CHSH} \quad (3.40)$$

$W_{CHSH}$  does not only determine whether a state is entangled or separable but also tests the local realism. By applying the Bell states(Eq. (2.14) - (2.17)),  $\text{tr}(W_{CHSH} \cdot \rho)$  fulfils the condition, Eq. (3.37), and violates Eq. (3.38). However, the entanglement witness based on Eq. (3.40) is not optimal, see Ref. [11].

## Chapter 4

# Part II: Experimental Tests

Since the correctness of quantum mechanics has been confirmed in a variety of experimental situations in, e.g., nuclear and atomic physics, the rather rare disagreement found by Bell seems to be a duty for many physicists to experimentally test because the spatially separate systems may be the greatest vulnerability of quantum physics.

In the past thirty years, a great number of Bell test experiments has been performed. In order to rule out the local, realistic hidden-variable theory, ideas were created to raise the equipment efficiencies with improving technology and to close the existing “loopholes.”

### 4.1 Requirement for general experimental tests

Until now, experimental results without any auxiliary assumptions don't exist. In the real-life experiments, the efficiency of the apparatus has to be considered, therefore a reasonable extension of the inequality is to implicate the apparatus efficiencies.

But generally, for a direct experimental violation, we experimentally require at least:

- A source of a discrete state system which can be detected with high efficiency.
- High purity of the state. From the viewpoint of quantum mechanics, at least a strong correlation of each pair has to be achieved.
- High analyzer efficiency of transmission to allow states and reject all nearby unwanted states.
- Very high efficiency of transmission/absorption of the spectrum filter.
- Locality: the adjustable values of the apparatuses have to be quickly changed, so that any kind of information transfer isn't possible. In other words, the space-like separation needs to be created.

Any absence of mentioned specifications will prevent the violation of Bell's theorem. The dependence of the experiment on these specifications is demonstrated by the following three cases:

- Case I: nearly ideal, the efficiencies of the apparatuses are near 1. In this case, a wide range violation can be found.
- Case II: entirely poor apparatus efficiency, which leads to flattened curve around 0. This is especially the case in low energy cascade photon experiments.
- Case III: weak correlation, impure states with depolarization or partially low efficiency of the apparatuses.

These cases are schematized in the following Fig. 4.1:

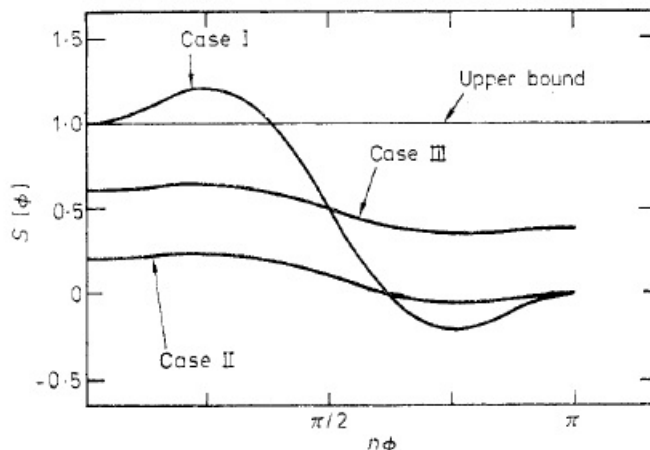


**Figure 4.1:** The curves are collected by violating the CH inequality with symmetry consideration  $S(\phi) \leq 1$ . (Ref. [10])

Indeed, as we see, an experimental violation of Bell's inequality has to be prepared carefully since the contrast of the curve observed in Fig. 4.1 drops down drastically at low efficiencies for partial experimental equipment.

By introducing an auxiliary assumption for rescaling the curve, the violation can be reached. Therefore measuring the efficiency coefficients of the experiment apparatuses becomes one of the most crucial points of all experiments. Besides improving technology, some of the experimental requirements can be fulfilled and some are still open. Since the experimental goal is to eliminate the possibility of an interpretation of the "hidden" variable theory by violating Bell's inequality, one has to consider additional conditions for the experiment, also called "loopholes." In other words, loopholes exist when we are not able to eliminate the theory of the "hidden" variable.

Let us in the following summarize the most critical additional assumptions (loopholes), which scientists have ever tried to eliminate:

- Einstein - locality: The distance between the two detectors should be large enough, so that any kind of exchange of information between the measuring systems below or equal to the speed of light isn't possible.
- Free choice: suppose a periodical procedure would reveal the information of the particles, we need a random choice machine to select the basis of measurement. Otherwise the information can be released before the measurement is executed.
- Fair sample: the detected samples represent the total ensemble of the particles emitted by the source. (The detection efficiency is always lower than 100% in an optical experiment. Calculation[8] shows that the violation doesn't hold for a detection efficiency below 82%.)

In the chapters below, I only restrict the content to optical experiments because of the remarkableness. Hence, a clear evolution of experimental verification is introduced. In the so called "three generations" of Bell experiments, the unexplored loopholes were step by step closed with modern methods.

## 4.2 The "First" Generation

The very first published Bell test experiment with entangled photons is performed by Stuart J. Freedman and John F. Clauser[14] in 1972. In their experiment, they measured the two photons emitted by the excited Calcium atoms at a cascade decay. By making the following assumptions:

- The two photons propagate as separated localized particles,
- A binary selection (transmission or no-transmission) measurement for each photon,
- The probability of detecting a photon is independent of transmission of the polarizers,

they were able to show a clear violation of Bell's inequality. The experimental setup is sketched in the Fig. 4.2. A calcium atom beam effused from a tantalum oven. The output of 227 nm wavelength of a deuterium arc lamp is focused on the Ca beam. After the resonance absorption, the Ca atoms are excited to the  $3d4p^1P_1$ . Only 7 % of the atoms, which do not decay directly back to the ground state, decay first of all to the  $4p^2\ ^1S_0$ . Before they reach the ground state, there exists an intermediate state  $4p4s^1P_1$ , see Fig. 4.3. Two photons of 551 nm and 422 nm were emitted during this

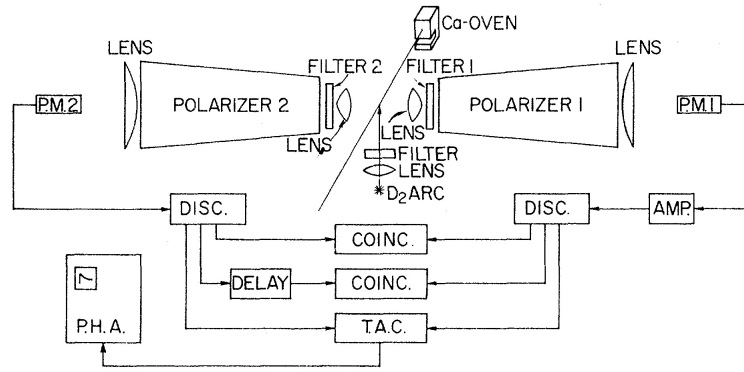


Figure 4.2: Schematic setup of Freedman and Clauser (Ref. [14])

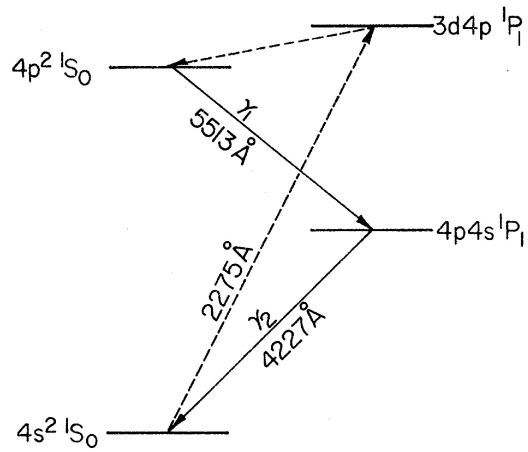


Figure 4.3: Calcium energy levels (Ref. [14])

cascade decay.

To avoid spherical aberrations which may influence the detection efficiencies, spherical primary lenses are used for each photon. Spectrum filters were also inserted for the selection and highly efficient piles-of-plates polarizers were used, which consist of thick glasses at Brewster's angle and can be manually adjusted. Finally, the photons were detected by the photon-multipliers detectors.

Measurement of the coincidence rate was executed by an electronic channel during a detection window of 8.1 ns. In a second channel, the delay time of 50 ns was caused consciously in order to measure the accidental coincidence, which will be abstracted from the primary data for the true coincidence. The whole system was cycled in 100 sec counting periods.

By applying the measurement results on a variation of CH-inequality with symmetry consideration,  $S \leq 0$ , they received the following result[14]:

$$S = 0.050 \pm 0.008 \quad (4.1)$$

This agreement between quantum mechanical prediction and experimental results enforces Bell's theorem.

In the following year, 1973, Holt and Pipkin[15] observed 567 nm and 404 nm photons produced from excited  $^{198}\text{Hg}$  by a 100 eV electron beam. But the result was in agreement with the inequality. After realizing this surprising result, they carefully searched for systematic errors in the experiment. Errors such as contamination of the source by isotopes, perturbation of external magnetic and electrical field, spurious counts of cosmic rays, stresses on the wall of the Pyrex bulb containing the electron gun mercury vapor, etc. falsified the measurement entirely. Even though the error was found, Holt and Pipkin never performed the experiment again.

In 1976, Clauser[16] repeated the experiment of Holt and Pipkin by using the same source and excitation mechanism. His very first result agreed with the results of Holt and Pipkin. After removing stress of improper set lens and 412 hours integration, the results were in excellent agreement with theoretical predictions.

The extremely remarkable precision of experimental arrangement characterizes the first generation of the Bell experiments. On the one hand, in spite of the open loopholes, Bell's theorem is found perfectly in accordance with the experiments. On the other hand, spaces of discussion about the validation still remain in the field.

### 4.3 The "Second" Generation

The main reason for naming this class of experiments the second generation is the consideration of the locality loophole in experiments employing visible photons. From 1981 to 1982, Alain Aspect et. al.[17] accomplished a series

of general tests of Bell's inequality.

The experiments of Alain Aspect et al. implied a straightforward transposition of EPRB-thought experiment and all of them possess a strong violation of the Bell's inequality.

Like Freedman and Clauser, they have experimented with visible photons correlated in their polarizations and produced by Ca cascade ( $J = 0 \rightarrow J = 1 \rightarrow J = 0$ ). The whole experiment was carried out for different distances between polarizers and the source. Differently from the experiment of Freedman and Clauser[14], Ca atoms are excited to upper energy level of  $4p^2 \ ^1S_0$  by two-photon absorption, which is realized by pumping the Ca atoms with two lasers with parallel polarization in reversed directions. These two lasers, a krypton laser of  $\lambda_k = 406$  nm and a dye laser of  $\lambda_d = 581$  nm, ensure the maximal emission rate of the source by feedback loops of the fluorescence signals, as we see in Fig. 4.4. Fluorescence occurs from  $4p^2 \ ^1S_0$  to  $4s4p \ ^1P_1$

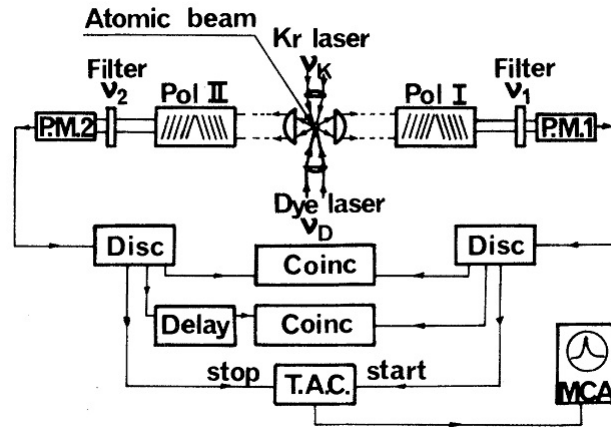


**Figure 4.4:** The setup arrangement of Aspect's experiment with two exciting lasers (Ref. [17])

for  $\lambda_1 = 551$  nm and from  $4s4p \ ^1P_1$  to  $4s^2 \ ^1S_0$  for  $\lambda_2 = 422$  nm, where the lifetime of the intermediate level lasts around 5 ns.

Two lenses collect the photons into "piles of plates" polarizers, separately. In order to eliminate the background noise, spectrum filters are set behind the polarizers. By using photon multipliers, the signals of both polarizers are amplified and the rate of coincidence within the 19 ns coincidence window is monitored by single-photon detectors. A second coincidence channel monitors the accidental coincidental rate with the time-delay of 100 ns between the signals. After analyzing the data, it declares a strong violation of the Bell's inequality, even after increasing the distance between the source and the polarizers up to 6.5 m.

In the further experiment, Aspect improved the setup in accuracy and re-

placed the “piles of plates” polarizers by beamsplitters, see Fig. 4.5. Another

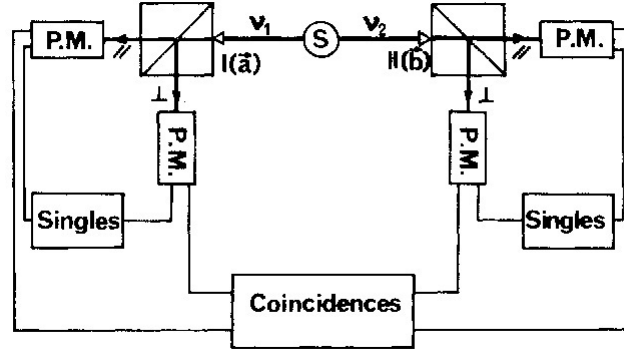


**Figure 4.5:** The setup arrangement of Aspect experiment with beamsplitters (Ref. [17])

benefit of the beamsplitter is proceed a fourfold coincidence measurement in a single run. With the fair sample assumption, for the first time CHSH-inequality is violated by applying the correlation function:

$$E(\vec{\alpha}, \vec{\beta}) = \frac{N_{++}(\vec{\alpha}, \vec{\beta}) + N_{--}(\vec{\alpha}, \vec{\beta}) - N_{-+}(\vec{\alpha}, \vec{\beta}) - N_{+-}(\vec{\alpha}, \vec{\beta})}{N_{++}(\vec{\alpha}, \vec{\beta}) + N_{--}(\vec{\alpha}, \vec{\beta}) + N_{-+}(\vec{\alpha}, \vec{\beta}) + N_{+-}(\vec{\alpha}, \vec{\beta})} \quad (4.2)$$

where  $N_{++}$  is the coincidence count of detecting + in both photon multipliers. Besides, an invariance of the total coincidence number under variation of the polarization orientations has also been experimentally proven.

Because in all of the experiments the setup is static, which hasn't fully excluded the locality assumption, Bell insisted that the setting needed to be changed during the flight of the particles.

The first attempt for the realization of the latter idea is to replace the polarizers by a setup involving a quick optical switching mechanism, acoustic-optical switch, followed by two different directions. Since the switch period is 10 ns and a intermediate level of cascade is 5 ns, the sum of them remains irrelevant to the maximal communication duration of 40 ns between the switches, a space-like separation seemed to be achieved.

The actual switching system, see Fig. 4.6, is based on the acoustic-optical effect by sonic standing wave in water. It follows that the light is transmitted completely when the amplitude of the standing wave vanished and deflected otherwise at the Bragg angle, where the amplitude of the acoustic wave causes a change of reflective index of the water. The transducers of the two switches were set in phase to 25 MHz. The result is also clearly in favor of the quantum mechanical prediction. They used another variation of CHSH-inequality,  $-1 \leq S \leq 0$ , which holds for all HVT. A clear violation

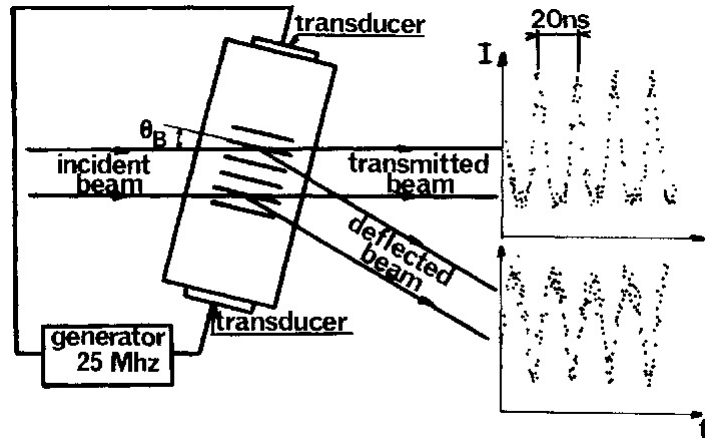


Figure 4.6: Acoustic-optical switches (Ref. [17])

yielded out[17]:

$$S = 0.101 \pm 0.020 \quad (4.3)$$

with a theoretical prediction of  $S_{QM} = 0.112$ . The additional assumptions which have to be made are sufficiently high detector efficiency and fair detected samples of all emitted pairs. Until this point, it seemed the locality loophole is eliminated at first.

#### 4.4 The “Third” Generation - G. Weihs, A. Zeilinger 1998

This experiment definitely implements the ideas behind the experiments of Alain Aspect et al.. In the experimenter’s view, the usage of the acoustic-optical switches, which is applied by a sinusoidal voltage, hadn’t successfully ruled out the locality assumption. The periodical change of the applied voltage could somehow be predicted after all. Furthermore, distances and switch frequency have been chosen unfortunately<sup>1</sup>, see Ref. [12, 13]. Thus communication at the speed of light or even slower than the speed of light could theoretically explain the obtained results.

For the first time, the experiment of G. Weihs[18] fully eliminated the locality assumption with entangled photons in their polarizations. In their experiment, the two detectors, so called “Alice” and “Bob,” were separated by a distance of 400 meters for the space-like separation. To prevent any communication obeying Einstein’s locality, the measurement duration was kept at 100 ns, which is clearly shorter than  $1.3 \mu s$ , the duration of the

<sup>1</sup>A. Zeilinger, Phys. Lett. IISA, 1 (1986)

communication between the detectors.

The entangled photons are produced by a BBO( $\beta$ -BaB<sub>2</sub>O<sub>4</sub>) negative uniaxial birefringent crystal ( $n_e < n_o$ ) with the type II spontaneous parametric down-conversion (SPDC - type II) pumped by a laser. SPDC - type II is a reverse process of the second harmonic generation (SHG), which is able to downconvert one pump photon ( $E = 2\hbar\omega_0$ ) in ex-ordinary polarization into two identical photons ( $E = \hbar\omega_0$ ), one in ordinary and the other in ex-ordinary polarization under the laws of conservation of energy and momentum.

However, the BBO crystal has a disadvantage. Due to birefringence of the crystal, a route difference exists for ordinary and ex-ordinary wave in the BBO ( $n_e < n_o$ ), called the “walk-off” effect. Because this effect can destroy the condition for the entanglement, compensating systems including the same cutting but thinner BBO are introduced to cancel the difference. One of the key elements of this experiment is the selection of an analyzer direction which completely processes unpredictably by a random number generator. The actual selection is caused by an electric-optical modulator, which changes the polarization of the light by applied voltage. In this experiment, a random number generator is responsible for the random change in voltage. In general, such a machine can be seen as a background noise generator. In this case, the basic idea is to send single photons of a weak light-emitting diode into a beamsplitter. Signals will be received either in one or in the other detector. Two photo-multipliers convert the weak signal into digital “0” or “1.” And finally, these signals are connected with a flipflop, as shown in Fig. 4.7. The output of the random number generator

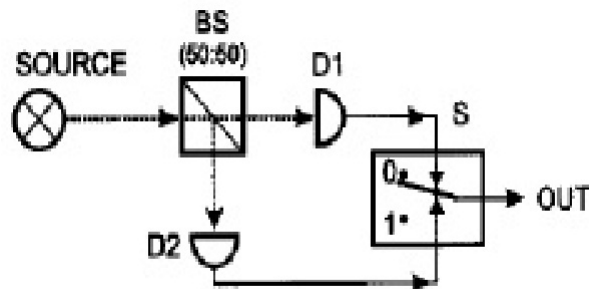


**Figure 4.7:** The basic idea of the quantum random number generator (Ref. [22])

controls the applied voltage of the electric-optical modulator, which is able to change the photon polarization within a defined range.

After measurement and calculation of the expectation values from coinci-

dence for the CHSH-inequality, a strong violation[18] of

$$S = 2.73 \pm 0.02 \tag{4.4}$$

agrees very well with quantum mechanical predictions.

It still seems unlikely, that the local, realistic theory can be completely abandoned because of other existing loopholes. In 2008, Salart et al.[23] enforced again the non-local argument with a separation of 18 km between the detectors in the Bell test experiment. In 2009, Ansmann et al.[24] seemed to overcome the greatest loophole, the detection loophole, with superconducting qubits, but the separation condition wasn't fulfilled.

## 4.5 Lab report

The present chapter contains a lab report of a self-made Bell test experiment in the framework of "Praktikum III: Quantenoptik" of the university of Vienna. It describes the basic experimental technique in alignment of optical elements. By assuming the locality and detection efficiency, we also successfully violate the CHSH-inequality. In conclusion, this experiment can only be considered as an introduction to quantum information experiments. But it surely awakes our interests in this field.

### 4.5.1 Experimental requirements

- BBO-crystal (Type II)
- 2 compensating BBOs (Type II)
- A Half-wave-plate
- A Pump laser (404 nm, max. 50 mW)
- 2 Polarizers
- 2 Detectors with single mode fiber coupling
- 2 Laserdiodes (630 - 680 nm, max 5 mW)
- Diverse optical components

### 4.5.2 Setup and execution

The key to every highly sensitive measurement is the setting. If the setup has been done carefully, the result will also be more acceptable. First of all, we have to keep one thing in mind, which is to take as much time as possible to do the setup. The construction of our experiment isn't very complicated, as shown in Fig. 4.8. The very first step is to set up the pump beam. To

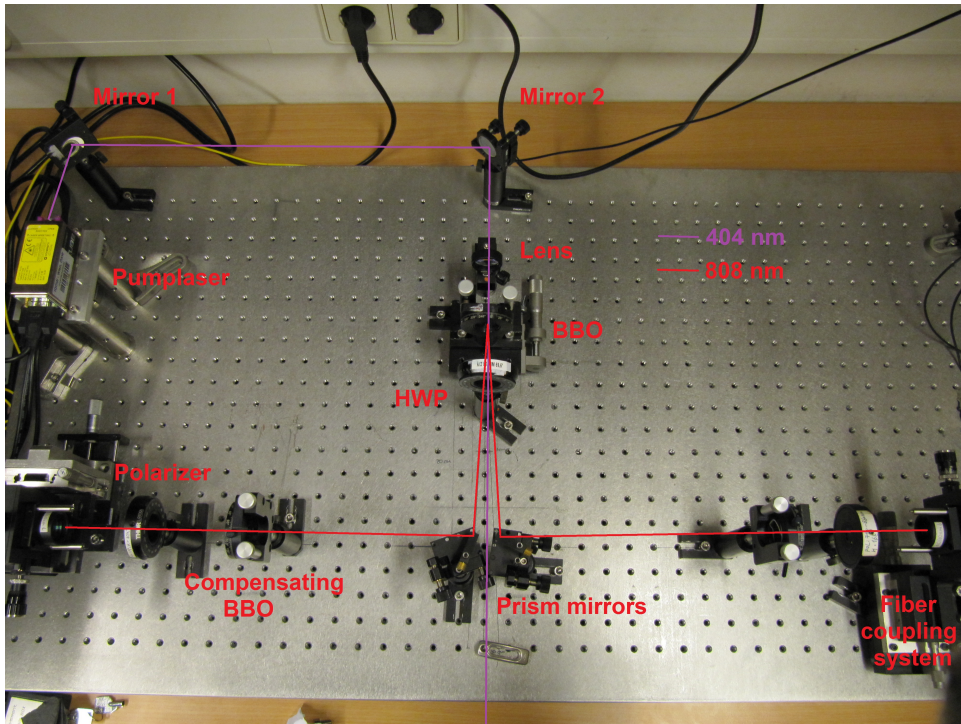


**Figure 4.8:** The setup: After two steering mirrors (M1,M2), the pump beam (404 nm, V-polarized) is focused into the BBO crystal (optical axis is in the vertical plane) by a lens of 6 cm focal length to create a pair of entangled photons (808 nm). The two 808 nm beams, which propagate along the lines which are  $3^\circ$  from the pump line horizontally, are deflected to left and right by two prism mirrors after passing through a half wave plate (HWP). Before coupling into the fiber, which connects with the detectors by a lens-system, each beam passes through a compensating BBO crystal and a  $808 \pm 10$  nm spectrum filter.

minimize the upcoming problems during the experiment, we have to keep the pump laser straight horizontal for the entire optical table and all optical components, such as the coupling system, should have the same height as the pump beam. Because of the fixed pump laser diode (404 nm), we need two reflecting mirrors for 404 nm, combined with two identical pinholes to freely adjust the beam height and make the beam parallel to the optical table. To have accurate alignment, the pinholes should have as much distance from each other as possible.

The most critical step is to set up the rest of optical components for down-converted beams, especially the fiber coupling systems. The key element of our detectors is the single mode fiber. Coupling a 808 nm beam into the fiber depends extremely on the incidence angle. We can't align the setup with the actual down-converted beams because the intensity is too low on the one hand and 808 nm isn't visible for human eyes on the other hand. Therefore we will send two 680 nm laser beams in the reverse direction of 808 nm beam from the fiber coupling system and try to make two "back tracing" laser beams overlap each other in the down-converting BBO crystal.

*Where to put the fiber coupling systems and how to make 680 nm and 808 nm beams collinear?*

First of all, the two detection arms must have the same length.

*How critical is the length difference between two detection arms?*

We know that the time interval for the detection of coincidence is set at 3 - 4 ns, which means photons detected at this time interval are interpreted as coincidence. The light will cover a distance of around 1 m within this time. Therefore as long as the difference between the detection arms is under 1 m, the mistakes are not critical. Even so, we still try to make the two arms symmetric.

As we know, the two 808 nm beams coming from the down-converting BBO have an included angle of  $6^\circ$ . Therefore we can calculate the exact positions to lead the beams into the fiber coupling system.

After the calculation, we mark the exact position for the BBO crystal above 15 cm away from the reflecting mirrors (M2) by a pinhole and have two prism mirrors 20 cm away from the BBO position. We place each fiber coupling system 40 cm away from the prism mirror symmetrically.

To fix the two 808 nm beams with an included angle of  $6^\circ$ , we also have constructed two special beam positioners with three pinholes (two side pinholes are for positioning the 808 nm beams and the middle one is for positioning the 404 nm one), as shown in Fig. 4.9, for fixing the 808 nm beams at positions 10 and 18 cm away from BBO crystal position respectively. Now we connect the 680 nm laser beams to the fiber coupling systems and adjust the prism mirrors to deflect 680 nm beams through the side pinholes on the two positioners. Thus the two 680 nm beams will overlap each other at the BBO crystal position.



**Figure 4.9:** Pinholes and beam positioners

We then remove the pinhole and insert BBO crystal at this position and adjust its optical axis in the vertical plane. To make the surface of the crystal orthogonal to the pump beam, we use the “back reflection” to adjust the BBO crystal. We put a pinhole in front of the crystal and have the pump beam pass through. Then we will see a reflection beside the pinhole. If the crystal is perfectly adjusted, the reflection will fall into the hole.

To increase the rate of down-converted photons, we need to focus the pump beam on the crystal. Therefore a lens with a focal length of 6 cm is put in front of the crystal. To avoid diverse optical aberrations, the pump beam has to go through the center of the lens perfectly. Otherwise the beam will be deflected. Finally, the compensating system is installed. It consists of a half-wave-plate and two compensating BBO crystals with half width but the same cutting of the down-converting BBO. The half-wave-plate is placed after the down-converting BBO crystal. The two compensating BBOs are placed in front of the fiber coupling systems and aligned by the “back reflection” method.

*How to find the optical axis of the half-wave-plate?*

At first, we need two polarizers illuminated by a 680 nm laser and let both polarized horizontally. Then, we put the HWP between these two polarizers and adjust the angle of the HWP until the out-coming light reaches a minimum. This is the right angle for the optical axis ( $45^\circ$  to the vertical) because the first polarizer makes the light horizontal and HWP turns it into vertical which is blocked by the second polarizer entirely.

We then remove the 680 nm beams and beam positioners and connect the detectors to the coupling systems. Now the system should be able to pro-

duce entangled photons.

Last but not least, we will couple 808 nm beams into the detectors.

After turning on the detectors and turning the pump laser power to 40 mW, we first try to find the maximum of photons by tuning the coupling system vertically and horizontally with the coarse adjustment on the X-Y translation stages. As soon as we find the maximum, we can be sure that we are close to the rings, the possible area of measurable 808 nm beam. We now insert the spectrum filters in front of the coupling systems to only allow 808 nm to sift through. In order to maximize the signal, we have to fine tune the X-Y translation stage again. As soon as we find a local maximal at one horizontal position, we change the X-micrometer a little bit and maximize the value by moving the Y-micrometer. If we iterate this procedure, we will slowly reach the global maximum by comparing all local maximums. Once the global maximum is reached, we will adjust the focus lenses in the coupling systems on Z-axis, to increase coupling efficiency. We call this procedure “walk-in.”

*How far are we from the intersection of the rings?*

Only at the intersection do we have as many horizontal photons as vertical. We can place a polarizer directly behind the compensating BBO and rotate it from  $0^\circ$  to  $360^\circ$  while we are fine tuning the coupling system on the X-Y-plane. Around the intersection, the difference between the maximum and the minimum with respect to the angle of polarizer will get smaller. While we are minimizing the difference we should also keep an eye on the coincidence rate. The rate of the single photons may drop down but the rate for coincidence is what we need. Now we need to make all five adjustments (two coarse and two fine adjustments on x-y-plane and one for the focus) on the coupling system to optimize the rate, which is the most sensitive part of tuning.

To demonstrate the violation of Bell’s inequality we need at least 50 coincidence per sec.

### 4.5.3 Results

When the system reaches a maximal rate of coincidence of 109 counts per second after the setup is optimized, we start to measure the Bell state, which the system produces.

To determine the state, we need to measure the state with at least two bases. According to the correlation of the Bell states, we can systematically preclude the possibilities for other states. The details can be seen in table 4.1.

For the first measurement we choose the H and V bases. A H polarizer is inserted behind the compensating BBO on the left detection arm. A V polarizer is placed symmetrically on the right detection arm. By varying the angle of the V polarizer step by step we measure the coincidence per

	H/V	+/-	R/L
$\phi^+$	1	1	-1
$\phi^-$	1	-1	1
$\psi^+$	-1	1	1
$\psi^-$	-1	-1	-1

**Table 4.1:** Correlation of the Bell states in all three bases. -1 denotes anti-correlation and 1 stands for correlation.

second, which is displayed on the detector.

Fig. 4.10 shows the coincidence rate as a function of relative angle between

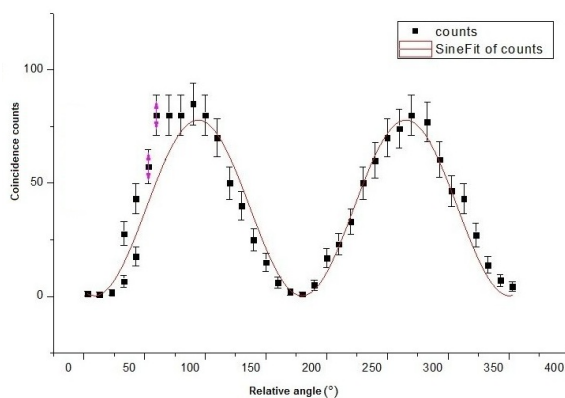


**Figure 4.10:** Points are the measured coincidence rates and the red line is the sine fitting curve.

the two polarizers.

As we see, the coincidence rate drops to the minimum when the relative angle is  $n \cdot 180^\circ$ . The rate is at its maximum when the polarizers are orthogonal to each other. That means that the measurement in H/V bases gives us anti-correlated results, which also help us to exclude the possibilities of the  $|\phi\rangle$ .

The visibility of the curve is

$$V_{H/V} = 98.75 \pm 0.47\%.$$

We execute the same measurement with the + and - bases, analogous to  $\pm 45^\circ$ . Here, the  $+45^\circ$  polarizer on the left arm is fixed and the  $-45^\circ$  polarizer on the right arm is rotated.

As it can be seen in Fig. 4.11, the coincidence rate is at maximum when the polarizers are orthogonal to each other again. The rate sinks to the minimum when the polarizers are parallel or anti-parallel. The visibility of

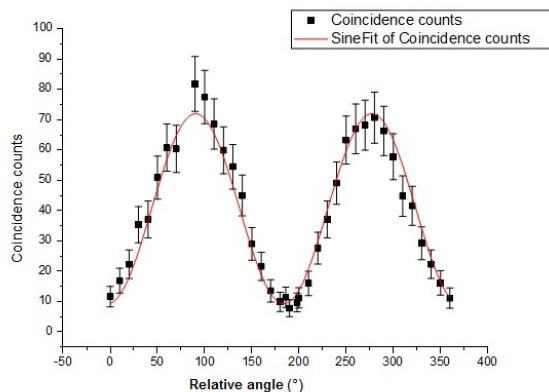


**Figure 4.11:** Points are the measured coincidence rates and the red line is the sine fitting curve.

the curve is

$$V_{+/-} = 82.59 \pm 0.24\%$$

From these two measurements on different bases, we come to the conclusion by using the table 4.1 that the system produces  $|\psi^-\rangle$ .

Now to demonstrate the violation of Bell's inequality, we calculate the Bell parameter, which is discussed at beginning:

$$S(\alpha, \beta, \alpha', \beta') := \left| E(\vec{\alpha}, \vec{\beta}) - E(\vec{\alpha}, \vec{\beta}') \right| + \left| E(\vec{\alpha}', \vec{\beta}') + E(\vec{\alpha}', \vec{\beta}) \right| \quad (4.5)$$

For the calculation of the expectation values in this formula, we measure the coincidence rates at the Bell angles,  $\alpha = 0^\circ$ ,  $\beta = 22.5^\circ$ ,  $\alpha' = 45^\circ$  and  $\beta' = 67.5^\circ$ , which will give us the maximal violation. We receive the table 4.2.

After analyzing and computing the data, we obtain:

	$\alpha=0$	$\alpha'=45$	$\alpha^\perp=90$	$\alpha'^\perp=135$
$\beta=22,5$	13	15	86	53
$\beta'=67,5$	62	22	17	68
$\beta^\perp=112,5$	61	65	14	31
$\beta'^\perp=157,5$	9	55	82	14

**Table 4.2:** Coincidence rate

$$S = 2.31 \pm 0.13$$

Here the uncertainty for the measurements is based on the uncertainty of the coincidence counts  $\sqrt{N}$ , which is given by the coherence state statistic, i.e., the laser photon statistic. ( $\sqrt{N}$  is also the standard deviation of the Poisson distribution for the Fock-statistics.)

#### 4.5.4 Discussion

In the last section, we have argued that the Bell state  $|\psi^-\rangle$  is produced. A formal way to determinate quantitatively the Bell state is to calculate the correlation function. Another way of determination is to compare the coincident curves with the reference[18].

As we see, our measurement results confirm our quantum mechanical expectation. Compared to the experimental values of G. Weihs, A. Zeilinger's experiment[18], it is just a small violation. Due to our high visibility in H/V basis we expected a stronger violation, but on the other hand the low visibility in +/- basis may distort the results.

In the calculation of the uncertainty, not only the uncertainty during setting the angle, but also the background noise as well as random coincidence should also be considered.

The weak violation definitely can be improved by choosing an integration time longer than one second. The violation can also be reinforced by generally raising the coincidence rates. In the experiment, the position of the focus of the pump beam in the BBO crystal will also affect the results. The compensating BBO are designed for down-converted photons produced in the middle of the down-converting BBO. If the laser isn't focused in the middle of the down-converting BBO, the compensating BBOs are not able to eliminate the "walk-off" effect for most of down-converted photons. This may play a role in raising the intensity of "walk-off-free" photons. In other words, there is still room for improvement.

## Chapter 5

# Conclusion

As one can see, Bell's theorem is surely proven in agreement with experiments with existing loopholes. In spite of this experimental verification of Bell's theorem, we still can't fully disprove the possibility of a local, realistic interpretation of quantum mechanical results. Even though diverse additional assumptions are ruled out, we have to admit that the assumption of a faithful representation of the whole emitted ensemble of the particles by the registered sample of photon pairs has to be made each time.

One may have the idea that Bell's theorem may probably be only valid for photons after reading this document. The fact is, the same results are yielded in experiments with protons, positrons, ions and even particles like Kaons and B-mesons of particle physics[27]. Still it remains a open question: Can we eliminate the local, realistic interpretation of quantum mechanics? For me, it is only a question of time and idea.

## Chapter 6

# Acknowledgement

I want to use this opportunity to mention many people who supported me writing this work. I would like to especially thank:

First of all, my adviser, Prof. R. A. Bertlmann, for his valuable suggestions. He never put me under any time pressure, so that this work can be written in my spared time.

My dad, Dr. Z. Cheng, for introducing me quantum optical experimental knowledge and for correcting this work.

A good friend of the Yale university, Nikolay Dinev, for correcting my English.

Ugur Sezer and David Hämmerle, for the interesting discussions during the Praktikum: Quanten Optik course.

And finally my family, for their unconditional support.

# List of Figures

3.1	EPRB: G. Weihs, Ph.D. Thesis, Ein Experiment zum Test der Bellschen Ungleichung unter Einsteinscher Lokalität . . .	10
3.2	Classical correlation: A. Peres, Quantum Theory: Concepts and Methods, Kluwer 1993 . . . . .	10
3.3	Bell experiment: J. F. Clauser and A. Shimony, Bell's theorem. Experimental tests and implications, Rep. Prog. Phys 41, 1881 (1978) . . . . .	15
4.1	Case analyse: J. F. Clauser and A. Shimony, Bell's theorem. Experimental tests and implications, Rep. Prog. Phys 41, 1881 (1978) . . . . .	21
4.2	Freedmann and Clauser: S. J. Freedman and J. F. Clauser, Experimental Test of Local Hidden-Variable Theories, Phys. Rev. Lett. 28, 938 (1972) . . . . .	23
4.3	Ca energy levels: S. J. Freedman and J. F. Clauser, Experimental Test of Local Hidden-Variable Theories, Phys. Rev. Lett. 28, 938 (1972) . . . . .	23
4.4	Aspect: A. Aspect, J. Dalibard, and G. Roger, Experimental Test of Bell's Inequalities Using Time-Varying Analyzers, Phys. Rev. Lett. 49, 1804 (1982) . . . . .	25
4.5	Aspect: A. Aspect, J. Dalibard, and G. Roger, Experimental Test of Bell's Inequalities Using Time-Varying Analyzers, Phys. Rev. Lett. 49, 1804 (1982) . . . . .	26
4.6	Acoustic-optical switches: A. Aspect, J. Dalibard, and G. Roger, Experimental Test of Bell's Inequalities Using Time-Varying Analyzers, Phys. Rev. Lett. 49, 1804 (1982) . . . . .	27
4.7	Random number generator: G. Weihs, Ph.D. Thesis, Ein Experiment zum Test der Bellschen Ungleichung unter Einsteinscher Lokalität . . . . .	28
4.8	Lab report setup: by author . . . . .	30
4.9	Pinholes: by author . . . . .	32
4.10	HV: by author with OriginLab . . . . .	34
4.11	+ -: by author with OriginLab . . . . .	35

# Bibliography

- [1] A. Einstein, B. Podolsky, N. Rosen: Can quantum-mechanical description of physical reality be considered complete?, Phys. Rev. 47 (1935), S. 777 - 780
- [2] N. Bohr, Can Quantum-Mechanical Description of Physical Reality be Considered Complete?, Physical Review, 48 (1935), S. 700.
- [3] J. S. Bell, On the Problem of Hidden Variables in Quantum Mechanics, Rev. Mod. Phys. 38, 447-452 (1966)
- [4] J. S. Bell, On the Einstein-Podolsky-Rosen Paradox, Physics 1, 195 (1964)
- [5] J. F. Clauser, M. A. Horne, A. Shimony and R. A. Holt, Proposed Experiment to Test Local Hidden-Variable Theories, Phys. Rev. Lett. 23, 880 (1969)
- [6] J. F. Clauser and M. A. Horne, Experimental consequences of objective local theories, Phys. Rev. D 10, 526 (1974)
- [7] B. Hiesmayr, script of theoretical physics, <https://www.univie.ac.at/physikwiki/index.php/Datei:Kapitel1.pdf> (June 2011)
- [8] A. Garg and N. D. Mermin, Detector inefficiencies in the Einstein-Podolsky-Rosen experiment, Phys. Rev. D 35, 3831 (1987)
- [9] A. Peres, Quantum Theory: Concepts and Methods, Kluwer 1993
- [10] J. F. Clauser and A. Shimony, Bell's theorem. Experimental tests and implications, Rep. Prog. Phys 41, 1881 (1978)
- [11] R. A. Bertlmann and P. Krammer, Optimal entanglement witnesses for qubits and qutrits, Phys. Rev. A 72, 052331 (2005)
- [12] R. A. Bertlmann, Bell's Theorem and the Nature of Reality, Found. Phys., Vol. 20, No. 10 (1990)

- [13] A. Zeilinger, Phys. Lett. HSA, 1 (1986)
- [14] S. J. Freedman and J. F. Clauser, Experimental Test of Local Hidden-Variable Theories, Phys. Rev. Lett. 28, 938 (1972)
- [15] R. A. Holt and F. M. Pipkin, Preprint Harvard University (1973)
- [16] J. F. Clauser, Experimental Investigation of a Polarization Correlation Anomaly, Phys. Rev. Lett. 36, 1223–1226 (1976)
- [17] A. Aspect, P. Grangier, G. Roger, Experimental Tests of Realistic Local Theories via Bell's Theorem Phys. Rev. Lett. 47(7), 460-463 (1981);  
A. Aspect, P. Grangier, G. Roger, Experimental Realization of Einstein-Podolsky-Rosen-Bohm Gedankenexperiment: A New Violation of Bell's Inequalities, Phys. Rev. Lett. 49, 91 (1982);  
A. Aspect, J. Dalibard, and G. Roger, Experimental Test of Bell's Inequalities Using Time-Varying Analyzers, Phys. Rev. Lett. 49, 1804 (1982)
- [18] G. Weihs, T. Jennewein, C. Simon, H. Weinfurter, A. Zeilinger Violation of Bell's Inequality Under Strict Einstein Locality, Phys. Rev. Lett. 81, 5039 (1998)
- [19] J. S. Bell, Bertlmann's Socks and the Nature of Reality, Journal de Physique 42 (1981)
- [20] R. A. Bertlmann, A. Zeilinger, Quantum [Un]speakables, Springer (2002)
- [21] D. Bouwmeester, A. Ekert, A. Zeilinger, The physics of quantum information, Springer (2000)
- [22] G. Weihs, Ph.D. Thesis, Ein Experiment zum Test der Bellschen Ungleichung unter Einsteinscher Lokalität
- [23] D. Salart, A. Baas, J. A. W. van Houwelingen, N. Gisin, and H. Zbinden, Spacelike Separation in a Bell Test Assuming Gravitationally Induced Collapses, Phys. Rev. Lett. 100, 220404 (2008)
- [24] J. M. Martinis et. al., Decoherence Dynamics of Complex Photon States in a Superconducting Circuit, Phys. Rev. Lett. 103, 200404 (2009)
- [25] C. Cohen-Tannoudji, B. Diu, F. Laloe, Quantenmechanik Band 1, 2, 4.Auflage (2009)
- [26] D. Bohm, Quantum Theory, New York, Prentice Hall (1951)
- [27] R. A. Bertlmann, Entanglement, Bell Inequalities and Decoherence in Particle Physics, arXiv:quant-ph/0410028 v1 (2004)